electronics

MDPI

Article

A Multi-Objective Design Optimization for a Permanent Magnet Synchronous Machine with Hairpin Winding Intended for Transport Applications

Mohammad Soltani *, Stefano Nuzzo, Davide Barater and Giovanni Franceschini

Department of Engineering Enzo Ferrari, University of Modena and Reggio Emilia, 41125 Modena, Italy; stefano.nuzzo@unimore.it (S.N.); davide.barater@unimore.it (D.B.); giovanni.franceschini@unimore.it (G.F.)
* Correspondence: mohammad.soltani@unimore.it

Abstract: Nowadays, interest in electric propulsion is increasing due to the need to decarbonize society. Electric drives and their components play a key role in this electrification trend. The electrical machine, in particular, is seeing an ever-increasing development and extensive research is currently being dedicated to the improvement of its efficiency and torque/power density. Among the winding methods, hairpin technologies are gaining extensive attention due to their inherently high slot fill factor, good heat dissipation, strong rigidity, and short end-winding length. These features make hairpin windings a potential candidate for some traction applications which require high power and/or torque densities. However, they also have some drawbacks, such as high losses at high frequency operations due to skin and proximity effects. In this paper, a multi-objective design optimization is proposed aiming to provide a fast and useful tool to enhance the exploitation of the hairpin technology in electrical machines. Efficiency and volume power density are considered as main design objectives. Analytical and finite element evaluations are performed to support the proposed methodology.

Keywords: hairpin windings; electrical machines; multi-objective optimizations; optimization

Citation: Soltani, M.; Nuzzo, S.; Barater, D.; Franceschini, G. A Multi-Objective Design Optimization for a Permanent Magnet Synchronous Machine with Hairpin Winding Intended for Transport Applications. *Electronics* **2021**, *10*, 3162. https://doi.org/10.3390/electronics10243162

Academic Editors: Tamás Orosz, David Pánek, Anton Rassõlkin and Miklos Kuczmann

Received: 25 November 2021
Accepted: 15 December 2021
Published: 18 December 2021

1. Introduction

Due to the ever-more stringent emission and efficiency requirements, there is currently a wide interest in the research and development of more electric vehicles. Traction applications are pushing the boundaries for high speed and power density with innovations in cores, magnets, and winding designs [1]. However, while higher speeds mean higher power for a given torque, they also result in additional losses in cores and windings, thus lowering the overall efficiency, and in structural challenges relative to the rotating components. Additionally, the relative distribution of these losses highly depends on the type of converter used to supply the machine.

In high power density traction applications, hairpin windings are widely spreading and currently seeing an ever-increasing interest in several documents [2–5]. In comparison to windings with round conductors, the end-winding length is shortened and, consequently, the DC copper loss is reduced [6]. Besides this end winding feature, the flat and "massive" shape of each hairpin leg reduces the DC copper loss compared to their round-wound counterpart. Hairpin windings achieve a higher fill factor compared to the round winding, thus obtaining higher current density and peak torque. In addition, in a series production context, a fully automated manufacturing process is possible, potentially reducing the associated costs [7].

On the other hand, being a recent technology, not much research is available on the design optimization of machines equipping this type of winding, whereas several studies focusing on optimization techniques have been proposed for electrical machines featuring random windings. For example, in [8], the analysis, design, and optimization of

a permanent magnet synchronous motor (PMSM) intended for a campus patrol electric vehicle were presented. Its optimization objectives included minimization of voltage harmonic content and torque ripple. The optimum stator inductances and resistance of a PMSM were calculated in [9] using a particle swarm optimization (PSO) method. Furthermore, the maximization of the flux-weakening region was pursued in [10], where a surface-mounted PMSM was optimized. In [11], the torque ripple of a PMSM under both transient state and steady-state conditions was minimized through an analytical solution. A multi-physics optimization program based on a multi-objective genetic algorithm was developed in [12], to achieve a trade-off solution among the electromagnetic, mechanical, and thermal aspects.

Regarding hairpin windings, a design optimization was carried out in [13], where the aim of the optimization study was that of reducing the torque ripple, while little attention was given to the most critical challenge of hairpin windings, i.e., the high copper losses at high-frequency operation. This is due to skin and proximity effects, where the feeding alternating current flows in a fraction of the conductor's cross section. These phenomena exacerbate at high frequency operations and result in an increase of the effective conductor resistance (and, thus, of losses) [3].

A simple motor design for traction applications was introduced in [14], but with no optimization strategy being implemented. In [15], an induction motor equipping hairpin winding was optimized aiming at a low cost, rare-earth free design. However, the number of hairpin layers in the slot was kept fixed, thus limiting the degrees of freedom of the design optimization. Additional work has been recently published on hairpin windings, but they focus either on modelling aspects (e.g., AC loss estimation [2]) or preliminary calculations [6] or sensitivity analyses [16].

Considering all the above, in this paper, the aim is to use dedicated optimization strategies for the design of an electrical machine with hairpin windings intended for a race car application. As a case study to investigate the above concepts, the surface mounted PMSM "roughly" designed in [17] is considered. The design achieved in [17] is based on a random winding stator, thus the initial aim of this work is to transform the random winding into a hairpin one, while the second step is to move from a "rough" machine design to an optimal one. To this purpose, two objective functions were selected: maximization of the volume power density and minimization of the power losses. These are indeed the most critical and conflicting figures to achieve when hairpin windings are involved. Before implementing the optimization process, first a sensitivity analytical study is carried out on the number of poles and slots per pole per phase. This led to define a starting machine design which is used to validate the analytical sizing approach through the finite element (FE) methodology. Once validated, the analytical tool is firstly used to perform a study on the parameters mostly affecting the selected objectives, and then to run the optimization to achieve an optimal solution. The use of the analytical sizing equations ensures a limited computation burden compared to numerical-based (e.g., FE) approaches.

2. Preliminary Design Process

2.1. Assumptions and Constraints

In [17], the whole propulsion system of a Formula SAE [18] car was designed, with a detailed focus on the propulsion motor being the case study of this paper. The selection of the system architecture, i.e., a two-motor layout implemented onto the rear non-steering axle, was based upon budget considerations. Additional constraints, such as the overall dimensions of the chassis and those imposed by the race regulations were accounted for. When it came to the motor torque-speed usage during an endurance event, the resulting reduced flux-weakening region led to select the popular surface-mounted PMSM layout as the most suitable for this application, also considering lower production costs in a customized case, compared to interior PM or synchronous reluctance machine layouts.

The Formula SAE car project must meet a series of technical constraints imposed by the regulation. These are summarized as follows:

- The diameter of the wheels must be $\geq$203.2 mm.
- The maximum power P required from the battery must not exceed 80 kW.
- The maximum allowed DC-link voltage V_{DC} must not exceed 600 V.
- There are no limitations concerning the number and the type of electric motors.

A summary of the choices done in [17] is listed in Table 1. These are used as starting points for re-designing the motor with hairpin conductors and applying an optimization strategy on it.

Table 1. Design choices and requirements.

Parameter	Condition
Motor topology	Surface-mounted PM
Motor's location	Rear-axle
Maximum torque to wheels	600 Nm
Reduction ratio	10
Motor rated torque	30 Nm
Base speed	12,740 rpm

The main design parameters of the machine obtained in [17], used as a benchmark here, are listed in Table 2. These are used as starting conditions for the analytical sizing tool implemented as the basis for the multi-objective optimization, and whose equations are reported in the next subsection.

Table 2. Motor design parameters.

Parameter	Value
Mechanical power P	40 kW
Line-to-line Voltage V	540 V
Surface current density J	13 A/mm^2
Airgap flux density B_{ag}	0.85 T
Maximum tooth flux density B_t	1.6 T
Maximum yoke flux density B_y	1.4 T
Linear current density A	70 A/mm
Targeted efficiency	95%

2.2. Machine Sizing Equations

The design process is initialized by defining some basic machine performance requirements, such as output power, speed, voltage, and desired efficiency [19]. The values of such input parameters are listed in Table 2. The second step is that of making some assumptions on the core materials and the cooling system, which are listed in Table 3, where also the main parameters used during the design process are described.

Table 3. Design choices and symbols.

Parameter	Value
Core material	M330-50A
PM material	N28AH
Cooling system	Natural convention
Stator winding	Distributed, full-pitch, single layer

Table 3. *Cont.*

Parameter	Symbol
Fill factor	k_{ff}
Outer rotor diameter [mm]	D
Axial length [mm]	L
PM span [deg]	α_{PM}
Number of phases	m
Number of slots-per-pole-per-phase	q
Pole pair number	p

Core materials and cooling system allow defining magnetic and electric loadings and the maximum flux density values allowed in the various parts of the motor. Assuming a number of phases m equal to 3, the slot number is calculated as $Q = q{\cdot}m{\cdot}2p$, and the number of turns per phase as $N = z_q{\cdot}q{\cdot}p$. Given the type of winding structure initially assumed, short pitch factor k_{cp} is equal to 1, while the distribution factor k_d is calculated using (1), where β is the slot pitch angle. The winding factor k_w is given by the product of k_{cp} and k_{d} [19].

$$k_d = \frac{\sin\left(\frac{q.\beta}{2}\right)}{q.\sin\left(\frac{\beta}{2}\right)} \tag{1}$$

Having preliminarily selected the D/L ratio, the starting point for the motor sizing is the torque expression given in (2). In (2) B is the RMS value of the fundamental harmonic B_{max} of the airgap flux density, which is obtained from (3) using the Fourier series decomposition of a square wave waveform that has amplitude B_{ag}. A is the RMS value of the linear current density. Equation (2) permits to find the values of D and L. Then, hypothesizing in the PMs the same flux density as in the airgap leveraging on Gauss' law, (4) can be used to determine the thickness l_m of the PMs. This means that the PMs are initially sized to meet the no-load requirements. In (4), B_r and μ_r are the residual flux density and relative permeability of the PMs [19].

$$T = \frac{\pi}{2} D^2 L B A \tag{2}$$

$$B_{max} = \frac{4B_{ag}}{\pi}.\sin\left(\frac{p\,\alpha_{PM}}{180}.\frac{\pi}{2}\right), \tag{3}$$

$$l_m = \frac{\mu_r l_g}{\frac{B_r}{B_{ag}} - 1}, \tag{4}$$

The total area $S_{\text{all slots}}$ to be dedicated to the three machine phases can be calculated using (5). Yoke thickness W_{y} and tooth width W_t can be calculated using (6) and (7), respectively. In (6), Φ_p is the physical flux per pole and B_y the maximum yoke flux density, whereas in (7) B_{avg} is the average airgap flux density, λ_s is the stator slot pitch and B_t is the maximum yoke flux density [19].

$$A = \frac{J.S_{\text{all slots}}.k_{\mathrm{ff}}}{\pi D} \tag{5}$$

$$W_y = \frac{\phi_p}{2B_y L} \tag{6}$$

$$W_t = \frac{B_{\mathrm{avg}}.\lambda_s}{B_t} \tag{7}$$

2.3. Power Losses

Besides these design aspects, the most crucial factor to consider when designing an electrical machine with hairpin windings is the AC Joule losses. In random windings

with stranded conductors, the AC losses can be neglected in the first approximation. In contrast, in hairpin windings, AC losses need to be carefully considered and determined. The DC resistance R_{DC} of a machine phase depends on the total length of one coil L_c, the number of turns in series N and parallel paths per phase, the cross-sectional area of the conductor S_c and the conductivity of the conductive material σ_c. Considering a uniform current distribution at any frequency in stranded conductors, the losses associated with the DC resistance are the only contribution to Joule losses. On the other hand, in hairpin conductors, skin and proximity effects and the ensuing AC losses are usually determined through the ratio between R_{AC} and R_{DC} [6]. For each layer k in the slot, this ratio (k_{Rk}) is determined using (8), where φ, ψ and ξ are expressed as in (9)–(11). In (11), h_{c0} and b_c are the height and width of the conductors, respectively, while b is the slot width, ω is the supply frequency, and μ_0 is the permeability of vacuum.

$$k_{Rk} = \varphi(\xi) + k(k-1)\psi(\xi) \tag{8}$$

$$\varphi(\xi) = \xi \frac{\sinh 2\xi + \sin 2\xi}{\cosh 2\xi - \cos 2\xi} \tag{9}$$

$$\psi(\xi) = 2\xi \frac{\sinh \xi - \sin \xi}{\cosh \xi + \cos \xi} \tag{10}$$

$$\xi = h_{c0} \sqrt{\frac{1}{2} \omega \mu_0 \sigma_c \frac{b_c}{b}} \tag{11}$$

Regarding iron losses, materials' suppliers usually give the loss density in W/kg, at specific frequency and flux density values. This includes both eddy current and hysteresis losses. Analytically, iron losses can be found by dividing the magnetic circuit of the machine into n sections, in which the flux density is constant. Once the masses $m_{Fe,n}$ of the different n sections are calculated from the volume density, the losses $P_{Fe,n}$ in these parts can be approximated as in (12). Here, $k_{Fe,n}$ are "loss" coefficients that, for a synchronous machine, can be imposed equal to 2 in the teeth and 1.6 in the yoke; P_{10} is the loss density at 1 T; $\widehat{B_n}$ is the maximum flux density in the n-th section [19]. The total power losses are determined using (13), where $P_{Cu_{DC}}$ and $P_{Cu_{AC}}$ are the DC and AC copper losses, respectively.

$$P_{Fe} = \sum_n k_{Fe,n} P_{10} \left(\frac{\widehat{B_n}}{1T} \right)^2 m_{Fe,n}, \tag{12}$$

$$P_{Tot\_losses} = P_{Fe} + P_{Cu_{DC}} + P_{Cu_{AC}} \tag{13}$$

2.4. Power Density

For the sake of completeness, the formula for the calculation of the volume power density is reported in (14). This is found through the ratio between the output power P and the machine volume Vol, which is defined once the main dimensions are all calculated.

$$P_{Density} = \frac{P_{out}}{Vol} \tag{14}$$

3. Optimization Process

As mentioned in Section 1, there are two objectives, i.e., the maximization of the volume power density (see (14)) and minimization of power losses (see (13)), which is equivalent to maximizing the efficiency. There are four input variable parameters, i.e., pole pair number, slot per pole per phase number, conductors' number in the slots (N), and motor's axial length. Additionally, several constraints must be met for the optimization process. Therefore, a Multi-Objective Evolutionary Algorithm (MOEA) could be used, which needs to set the weight of the input parameters based on their effect on the two objectives, and a starting point for initializing the first population. Using the equations introduced in

Section 2, a sensitivity analysis is first carried out to understand the dependence of the two objectives on the four variable parameters.

The MOEA expects a single fitness value with which to perform the selection. Additional processing is sometimes required to transform MOEA solutions' fitness vectors into a scalar. Its sequential task decomposition includes initialized population, fitness evaluation, which has a sub-level as vector transformation, recombination, mutation, and selection [20]. Figure 1 shows these decomposition tasks in five sections which has the main loop for selecting the data between the third and fifth levels.

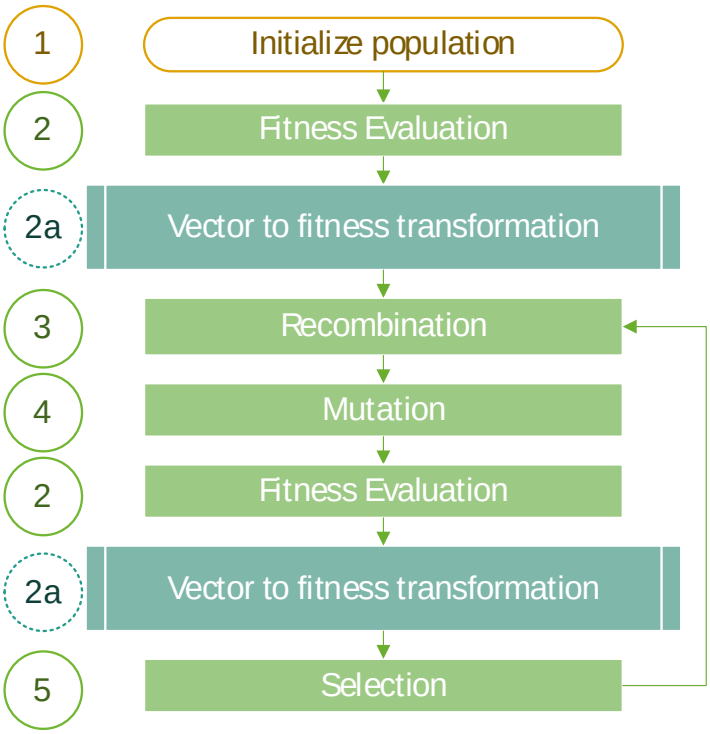

Figure 1. Sequential task decomposition for MOEA.

Regarding the constraints, first, the tooth width is imposed greater than 1.6 mm for structural reasons. Secondly, the loss density B_{10} at 1 T used in (12) for iron loss calculation is updated during optimization as it depends on frequency. Thirdly, to make the evaluation of the optimization objectives consistent, the inverse of the power density is considered, so that both the objectives must be minimized. Assuming to keep the frequency lower than 1 kHz as per [17], the maximum pole number should not exceed 8. Due to the dimensional limitations in terms of length and axial diameter, as well as the constraint on the tooth width, the maximum q is kept lower than 8. The axial length is varied between 10 mm and 100 mm. With an axial length higher than 100 mm the motor's diameter becomes less than 325 mm, resulting in a tooth width < 1.6 mm even with $q = 1$. The last constraint is on the maximum RMS value of the line-to-line voltage (see Table 2), which is limited by the maximum battery voltage (see Section 2.1). Another constrained value is the number of conductors per slot, which must be necessarily even due to the hairpin winding characteristics. A summary of the constraints is listed in (15)–(18).

$$2 \leq 2p \leq 8 \tag{15}$$

$$1 \leq q \leq 8 \tag{16}$$

$$10 \text{ mm} \leq L \leq 100 \text{ mm} \tag{17}$$

$$V_{L-L} \leq 540 \text{ V} \tag{18}$$

4. Results

4.1. Preliminary Sensitivity Analysis and Validation of the Analytical Model

Before using the analytical model for optimization purposes, it needs to be validated against the more accurate FE method. Once validated, it can be safely used for optimizations, thus saving computation time as opposed to FE. An initial sensitivity analysis could be carried out varying the number of poles and slots per pole per phase while keeping the other parameters constant. The sensitivity analysis results are illustrated in Figure 2, where power losses and volume power density are taken as indicators to suitably select q and p. The best solution is achieved with $p = 4$ and $q = 2$. The selected p-q combination represents the best trade-off in terms of maximum power density and minimum power losses. In fact, only two machines (referred to as "A" and "B" in the figure) achieve higher power density values, but these feature much larger losses (by 8.9% and 23.9%, respectively).

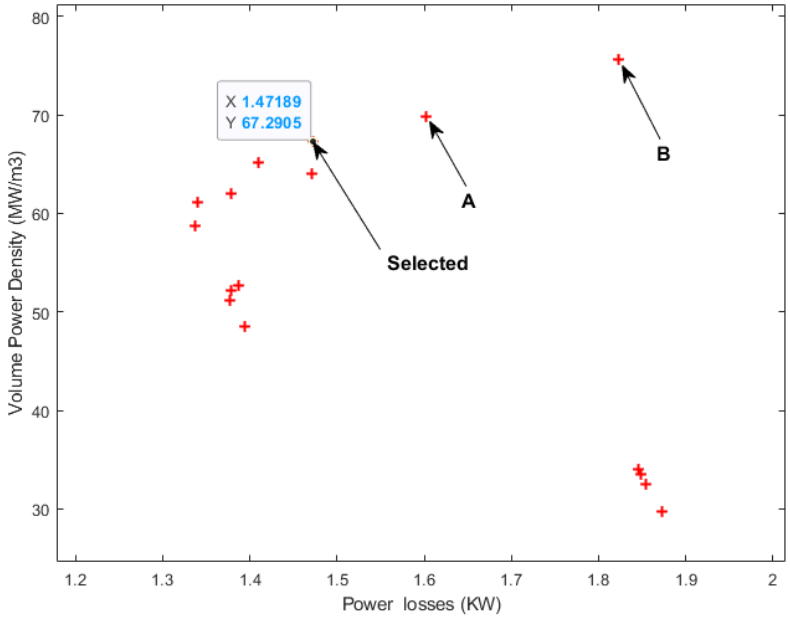

Figure 2. Preliminary sensitivity analysis.

The dimensions analytically obtained are used to build the machine geometry and a corresponding model within the FE-based software MagNet. Figure 3 shows the FE model of the motor, enriched with a flux density map and field lines distribution. Figure 4 plots the output torque obtained with the currents in phase with the corresponding back electromotive forces, with an average value equal to 30.1 Nm being obtained. This matches well the torque value of 30 Nm assumed in the analytical sizing. Besides the torque, the analytical and FE no-load voltage and flux density values in the various parts of the motor are compared. Figure 5 shows a comparison between the fundamental harmonic of the line-to-line voltage (red line) obtained from FE simulations and the corresponding sinusoidal waveform assumed for the analytical sizing (in green), with an error lower than 1% being achieved. For completeness, the FE voltage waveform evaluated via FE is also observed in Figure 5. In addition, Figure 6 illustrates the flux densities in the airgap and the main iron parts of the motor, with the blue lines referring to FE results and the red text relative to the analytical assumptions (see Table 2). Good matching is observed, with an error ranging from 3% to 8%, thus allowing to conclude that the analytical sizing equations, although suitable for preliminary sizing only, can be safely used for optimization purposes.

In the next subsection, the effect of some machine parameters on power density and power losses are investigated before proceeding with the optimization. This study allows weighting any of the input parameters in the multi-objective optimization process which will be the focus of Section 4.3.

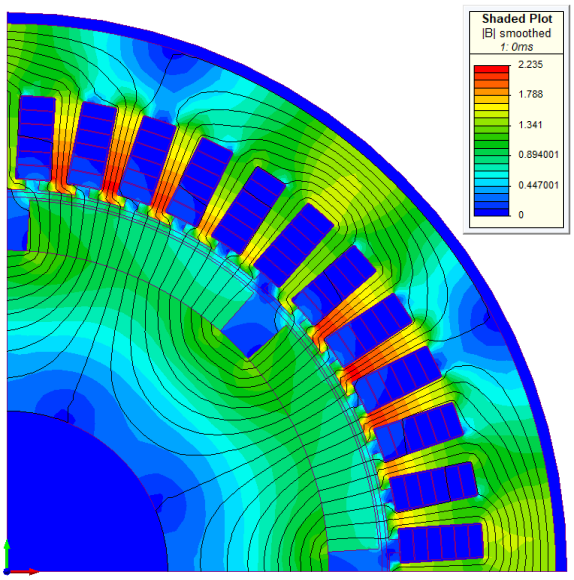

Figure 3. FE one pole pair model of the motor with the hairpin winding, highlighting flux density map (T) and field lines distribution at full-load operation.

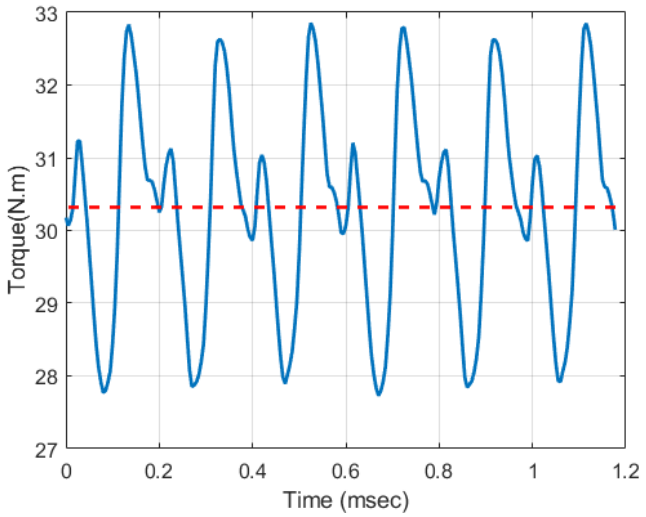

Figure 4. Output torque (in blue) and its average value (in red) obtained via FE analysis.

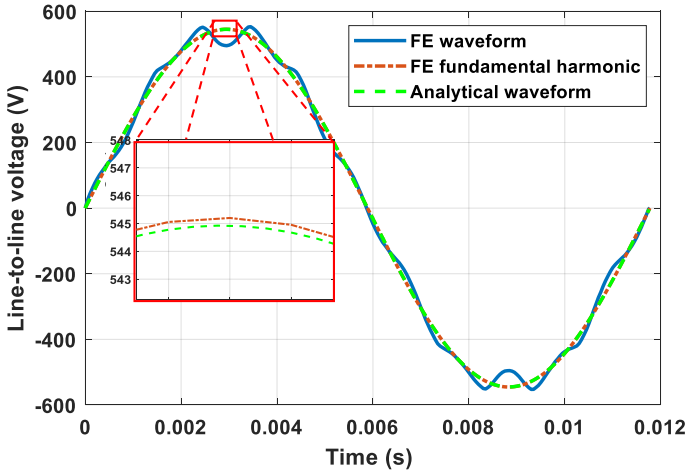

Figure 5. FE no-load line-to-line voltage (in blue) and its fundamental harmonic (in red) vs. analytical no-load line-to-line voltage (in green).

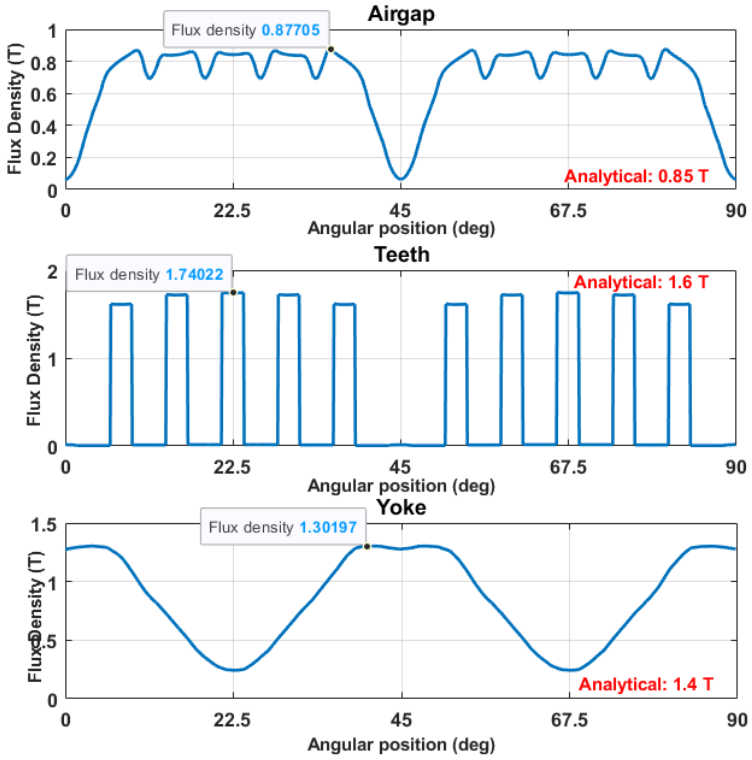

Figure 6. Comparison in terms of flux density in the airgap, teeth, and yoke.

4.2. Effective Parameters

Considering the analytical equations reported in Section 2.2, it is clear that several parameters can be utilized to achieve the main design objectives of this work, i.e., power density maximization and power losses minimization. Thus, a sensitivity analysis is performed. While the results of this study can vary depending on the power range, the geometrical and magnetic features, the airgap thickness, etc., of the PMSM motor under analysis, for the case study considered in this paper the sensitivity study can provide useful information for a first exploration of weight allocation during optimization. Assuming the hairpin motor of the previous section as the benchmark, the parameters used for the sensitivity study are normalized over the corresponding values of the benchmark machine. Figures 7 and 8 show the total power losses and volume power density for the four input parameters, i.e., pole pair number, slot per pole per phase number, conductor per slot number, and axial length. These parameters are changed "1-by-1" in this first exploration. All the curves meet at 1 p.u., corresponding to the benchmark machine. All the parameters have a non-negligible effect on both power losses (Figure 7) and power density (Figure 8). According to the methodology described in [20], the weight of each input parameter to be imposed in the optimization can be found through these figures. Using a coefficient equal to 1 for N, the pole pair number, the slot per pole per phase number and the axial length feature coefficients equal to 1.38, 1.1 and 1.15, respectively.

4.3. MOEA Results and Comparison

Regarding the mentioned sequential task decomposition of the optimization method (see Figure 1), before any mutation, the constraints (15)–(18) should be carefully considered. After running the optimization algorithm using 500 generations and 50 individuals per generation, the Pareto front shown in Figure 9 is finally obtained, where the last 50 designs are observed. Every sequential task of the optimization process shown in Figure 1 has been implemented in Matlab environment.

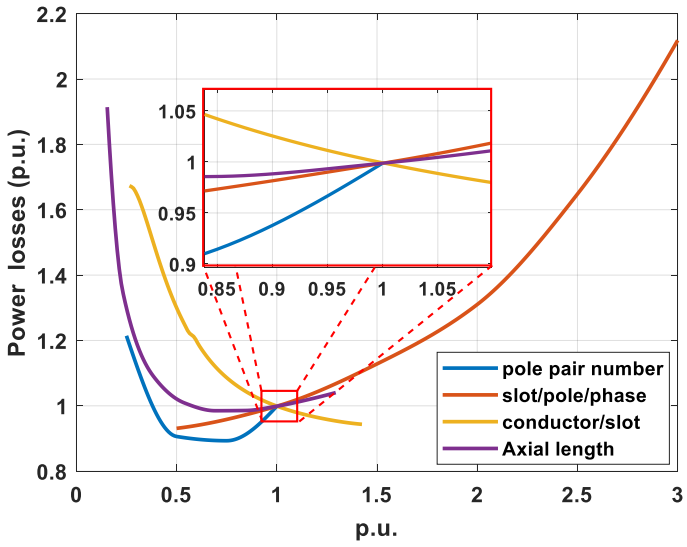

Figure 7. Effect of the input parameters on the total power losses.

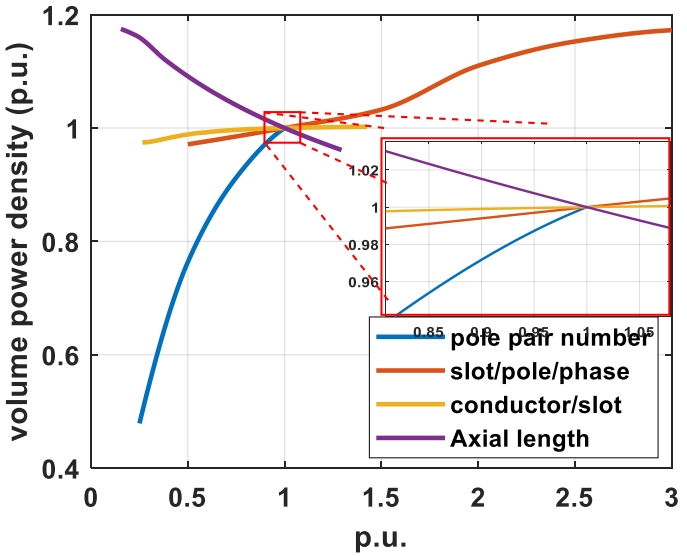

Figure 8. Effect of the input parameters on the volume power density.

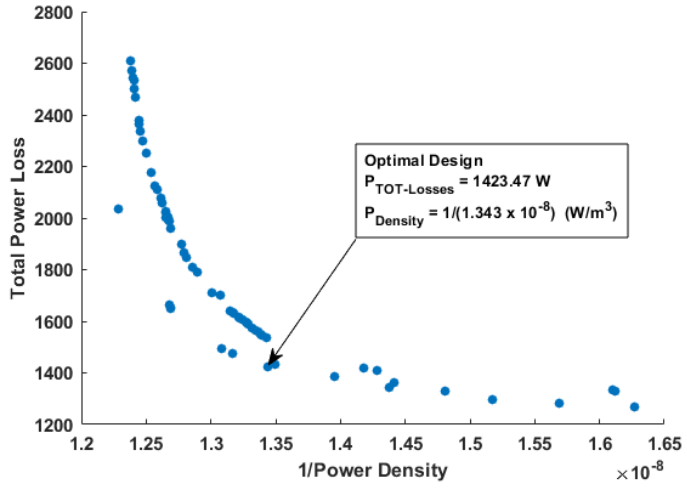

Figure 9. The final Pareto front with the final optimum point.

The optimal machine design is also highlighted in Figure 9, and its geometry is illustrated in Figure 10b, whereas in Figure 10a the machine design resulting from the first sensitivity analysis is shown for the sake of comparison. Table 4 compares the analytical results obtained for the motor with round winding designed in [17], the motor with hairpin winding resulting from the first sensitivity analysis, and the optimum one. With a focus on the motors with hairpin windings, the main indexes such as efficiency, volume power density, volume torque density, and power losses have been improved by 0.15%, 10.55%, 12.3%, and 3.4%, respectively. For completeness, the full-load output torque of the optimum motor obtained using FE is reported in Figure 11, with the mean value being highlighted in red and equal to 30.2 Nm.

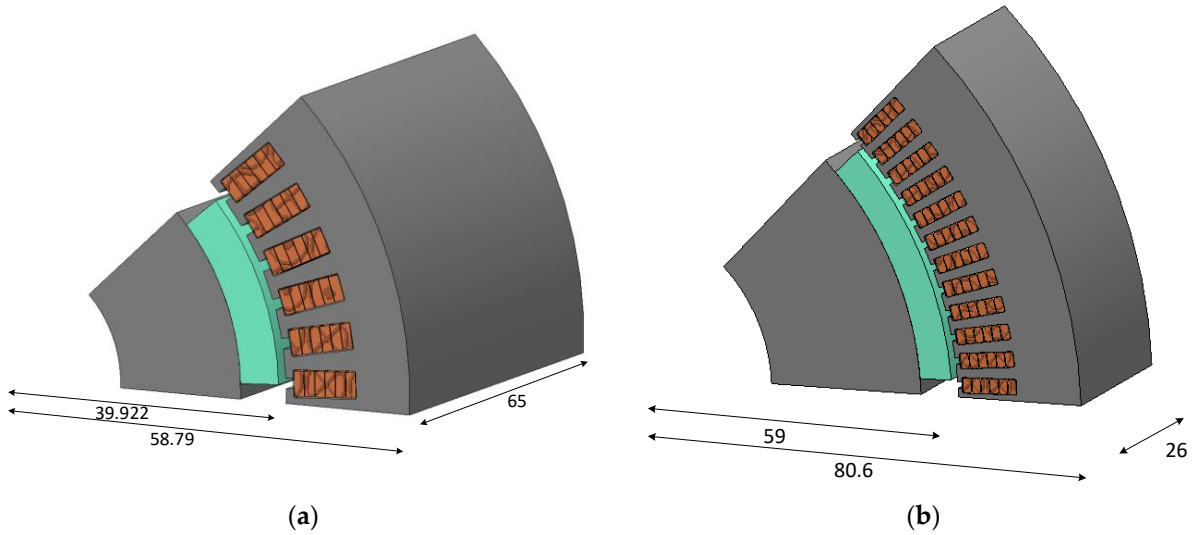

Figure 10. Comparison between the geometries of (**a**) the first analyzed motor and (**b**) the optimal motor.

Table 4. Summarizing comparison among the benchmark motor [17], the hairpin motor obtained through the first sensitivity analysis and the optimum hairpin motor.

Parameters	Round Winding	Hairpin 1st Design	Hairpin Optimal Design	Improvement
pole number	6	8	8	-
slot/pole/phase	1	2	4	-
axial length	65	65	26	-
conductors/slot	11	6	6	-
rotor radius	45	39.922	59	-
Tooth width	10	2	1.635	-
Yoke thickness	14	7.7	13.35	-
outer radius	85	58.79	80.6	-
Fill factor	60%	85%	85%	-
Peak current (A)	140	80.56	63.7	-
Torque ripple (%)	16%	17%	8.97%	9.03%
Power loss (kW)	2	1.47	1.42	10.55%,
Efficiency	95.2%	96.45%	96.6%	0.15%
volume power density (MW/m^3)	16.75	67.3	74.4	12.3%
volume torque density (kNm/m^3)	13.21	49.65	55.76	3.4%

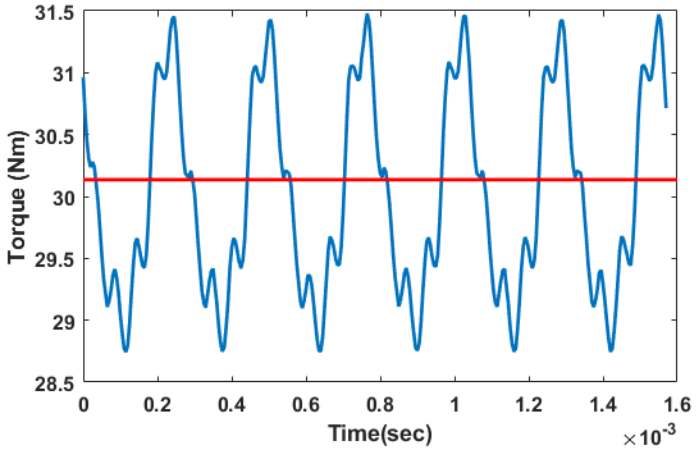

Figure 11. Output torque of the optimum motor.

5. Conclusions

In this paper, a fast and accurate optimization tool was introduced for optimal exploitation of hairpin technologies in electrical machines intended for traction applications. The optimization tool is aimed at maximizing power density and efficiency, which are key figures for the application at hand. In addition, given the challenges featured by hairpin conductors at high-frequency operations, these two objectives are rather conflicting, thus making the machine design complex. The optimization strategy, based first on a "one-by-one" sensitivity study and then on the application of a multi-objective evolutionary algorithm, proved that these two objectives can be pursued and achieved simultaneously, with excellent performance enhancement being obtained.

As a benchmark case study, a surface-mounted PMSM equipping random windings and previously designed for a Formula SAE car was considered. Therefore, the first exercise consisted of replacing the random winding with hairpin conductors. A preliminary sizing was first carried out based on the requirements of the application at hand. Then, the analytical sizing tool was validated against FE evaluations, with a maximum error of ≈8%, thus making the analytical equations a safe means for the optimization procedure. A sensitivity analysis was performed to suitably weight the optimization input parameters and, finally, the optimization algorithm was run. The optimal motor, which was selected for comparative purposes against the benchmark motor with random windings and a non-optimal hairpin motor, showed very promising results and significant performance improvements. In particular, the main indexes such as efficiency, volume power density, and power losses, were improved by 0.15%, 10.55%, and 3.4%, respectively.

Author Contributions: Conceptualization, M.S. and S.N.; methodology, M.S. and S.N.; software, M.S.; validation, M.S., S.N. and D.B.; formal analysis, M.S.; investigation, M.S.; resources, M.S.; data curation, M.S.; writing—original draft preparation, M.S.; writing—review and editing, S.N.; visualization, M.S.; supervision, S.N., D.B. and G.F.; project administration, D.B. and G.F.; funding acquisition, S.N., D.B. and G.F. All authors have read and agreed to the published version of the manuscript.

Funding: This research received no external funding.

Conflicts of Interest: The authors declare no conflict of interest.

References

1. Zhao, Y.; Li, D.; Pei, T.; Qu, R. Overview of the rectangular wire windings AC electrical machine. *CES Trans. Electr. Mach. Syst.* **2019**, *3*, 160–169. [CrossRef]
2. Arzillo, A.; Nuzzo, S.; Braglia, P.; Franceschini, G.; Barater, D.; Gerada, D.; Gerada, C. An Analytical Approach for the Design of Innovative Hairpin Winding Layouts. In Proceedings of the International Conference on Electrical Machines (ICEM), Gothenburg, Sweden, 23–26 August 2020; pp. 1534–1539.

3. Nuzzo, S.; Barater, D.; Gerada, C.; Vai, P. Hairpin Windings: An Opportunity for Next-Generation E-Motors in Transportation. *IEEE Ind. Electron. Mag.* **2021**, 2–10. [CrossRef]
4. Islam, S.; Husain, I.; Ahmed, A.; Sathyan, A. Asymmetric Bar Winding for High-Speed Traction Electric Machines. *IEEE Trans. Transp. Electrif.* **2019**, *6*, 3–15. [CrossRef]
5. Sculiller, F.; Zahr, H.; Semail, E. Maximum Reachable Torque, Power and Speed for Five-Phase SPM Machine With Low Armature Reaction. *IEEE Trans. Energy Convers.* **2016**, *31*, 959–969. [CrossRef]
6. Soltani, M.; Nuzzo, S.; Barater, D.; Franceschini, G. Considerations on the Preliminary Sizing of Electrical Machines with Hairpin Windings. In Proceedings of the 2021 IEEE Workshop on Electrical Machines Design, Control and Diagnosis (WEMDCD), Modena, Italy, 8–9 April 2021; pp. 46–51.
7. Popescu, M.; Goss, J.; Staton, D.A.; Hawkins, D.; Chong, Y.C.; Boglietti, A. Electrical Vehicles—Practical Solutions for Power Traction Motor Systems. *IEEE Trans. Ind. Appl.* **2018**, *54*, 2751–2762. [CrossRef]
8. Sun, X.; Shi, Z.; Lei, G.; Guo, Y.; Zhu, J. Analysis and Design Optimization of a Permanent Magnet Synchronous Motor for a Campus Patrol Electric Vehicle. *IEEE Trans. Veh. Technol.* **2019**, *68*, 10535–10544. [CrossRef]
9. Hernandez, O.S.; Morales-Caporal, R.; Rangel-Magdaleno, J.; Peregrina-Barreto, H.; Hernandez-Perez, J.N. Parameter Identification of PMSMs Using Experimental Measurements and a PSO Algorithm. *IEEE Trans. Instrum. Meas.* **2015**, *64*, 2146–2154. [CrossRef]
10. Dang, L.; Bernard, N.; Bracikowski, N.; Berthiau, G. Design Optimization with Flux Weakening of High-Speed PMSM for Electrical Vehicle Considering the Driving Cycle. *IEEE Trans. Ind. Electron.* **2017**, *64*, 9834–9843. [CrossRef]
11. Feng, G.; Lai, C.; Kar, N.C. An Analytical Solution to Optimal Stator Current Design for PMSM Torque Ripple Minimization With Minimal Machine Losses. *IEEE Trans. Ind. Electron.* **2017**, *64*, 7655–7665. [CrossRef]
12. Zhao, W.; Wang, X.; Gerada, C.; Zhang, H.; Liu, C.; Wang, Y. Multi-Physics and Multi-Objective Optimization of a High Speed PMSM for High Performance Applications. *IEEE Trans. Magn.* **2018**, *54*, 1–5. [CrossRef]
13. Jung, D.S.; Kim, Y.H.; Lee, U.H.; Lee, H.D. Optimum Design of the Electric Vehicle Traction Motor Using the Hairpin Winding. In Proceedings of the 2012 IEEE 75th Vehicular Technology Conference (VTC Spring), Yokohama, Japan, 6–9 May 2012. [CrossRef]
14. Xue, S.; Michon, M.; Popescu, M.; Volpe, G. Optimisation of Hairpin Winding in Electric Traction Motor Applications. In Proceedings of the IEEE International Electric Machines & Drives Conference (IEMDC), Hartford, CT, USA, 17–20 May 2021; pp. 1–7. [CrossRef]
15. Riviere, N.; Villani, M.; Popescu, M. Optimisation of a High Speed Copper Rotor Induction Motor for a Traction Application. In Proceedings of the IECON 2019—45th Annual Conference of the IEEE Industrial Electronics Society, Lisbon, Portugal, 14–17 October 2019; Volume 1, pp. 2720–2725. [CrossRef]
16. Preci, E.; Gerada, D.; Degano, M.; Buticchi, G.; Gerada, C.; Nuzzo, S.; Barater, D. Hairpin Windings: Sensitivity Analysis and Guidelines to Reduce AC Losses. In Proceedings of the 2021 IEEE Workshop on Electrical Machines Design, Control and Diagnosis (WEMDCD), Modena, Italy, 8–9 April 2021; pp. 82–87. [CrossRef]
17. Devito, G.; Nuzzo, S.; Barater, D.; Franceschini, G.; Papini, L.; Bolognesi, P. Design of the Propulsion System for a Formula SAE racing car based on a Brushless Motor. In Proceedings of the IEEE Workshop on Electrical Machines Design, Control and Diagnosis (WEMDCD), Modenta, Italy, 8–9 April 2021; pp. 318–324.
18. Formula SAE Rules 2021 Version 1.0. Available online: www.fsaeonline.com/cdsweb/gen/DocumentResources.aspx (accessed on 19 November 2021).
19. Pyrhonen, J.; Jokinen, T.; Hrabovcova, V. *Design of Rotating Electrical Machines*; John Wiley & Sons Ltd.: Chichester, UK, 2013.
20. Coello, C.A.C.; Lamont, B.G.; Van Veldhuizen, A. *Evolutionary Algorithms for Solving Multi-Objective Problems*; Springer: New York, NY, USA, 2007; Volume 5.